Article ID:0253-2778(2016)05-0431-08

$\gamma\gamma$ physics and transition form factor measurements at KLOE\KLOE-2

GAUZZI P. (for the KLOE-2 Collaboration)

(*Dipartimento di Fisica, Università La Sapienza e INFN, Sezione di Roma, Rome I*-00185, *Italy*)

Abstract: The KLOE results on the measurement of the transition form factors of the η and π^0 mesons in ϕ Dalitz decays are presented, and the determination of the $\Gamma(\eta\to\gamma\gamma)$ in $\gamma\gamma$ collisions is also reported. The prospects for $\gamma\gamma$ physics of the new data-taking, started in November 2014 with the upgraded detector, are reviewed.

Key words: gamma-gamma physics; transition form factors; electron-positron collider

CLC number: O572.3 **Document code**: A doi:10.3969/j.issn.0253-2778.2016.05.011

Citation: GAUZZI P. $\gamma\gamma$ physics and transition form factor measurements at KLOE\KLOE-2[J]. Journal of University of Science and Technology of China, 2016,46(5):431-438.

KLOE 和 KLOE-2 实验上双光子物理和跃迁形状因子的测量

GAUZZI P.(KLOE-2 合作组)

(罗马大学物理系,罗马 I-00185,意大利)

摘要:介绍 KLOE 实验 ϕ 介子达利兹衰变中 $\eta|\pi^0$ 介子的跃迁形状因子的测量结果以及在 $\gamma\gamma$ 碰撞中$\eta|\gamma\gamma$衰变宽度的测定.升级后的探测器从 2014 年 11 月开始取数,评述了双光子物理的前景.

关键词:双光子物理;跃迁形状因子;正负电子对撞机

0 Introduction

The KLOE Collaboration took data from 2001 to 2006 at the Frascati ϕ-factory DAΦNE, collecting about 2.5 fb^{-1} at the peak of the $\phi(1020)$, and 250 pb^{-1} off-peak, mainly at $\sqrt{s}=1$ GeV. In 2008 a new interaction scheme for DAΦNE has been adopted, aiming at an increase in luminosity. Following this successful test, a new data-taking campaign of the KLOE experiment (KLOE-2 in the following) with an upgraded detector has been proposed[1]. The DAΦNE commissioning for the KLOE-2 data-taking started in 2010. In December 2012 the machine was shut down to install the new beam-pipe with new detectors in KLOE. In July 2013, after the completion of the installation, the machine commissioning was resumed. The KLOE-2 data taking started in November 2014, with the goal to collect at least 5 fb^{-1} of integrated luminosity in 2~3 years. Until June 2015 DAΦNE had provided 1 fb^{-1} of luminosity, which has been collected by

Received:2015-11-27;**Revised**:2016-04-20

Biography:GAUZZI P., male, born in 1963, PhD. Research field: high energy physics. E-mail: paolo.gauzzi@roma1.infn.it

KLOE-2 with an efficiency of about 80%, as shown in Fig. 1. During this period the DAΦNE peak luminosity was about $2\times10^{32}\,\mathrm{cm}^{-2}\cdot\mathrm{s}^{-1}$, and the integrated luminosity collected in a day was about 10 pb^{-1}.

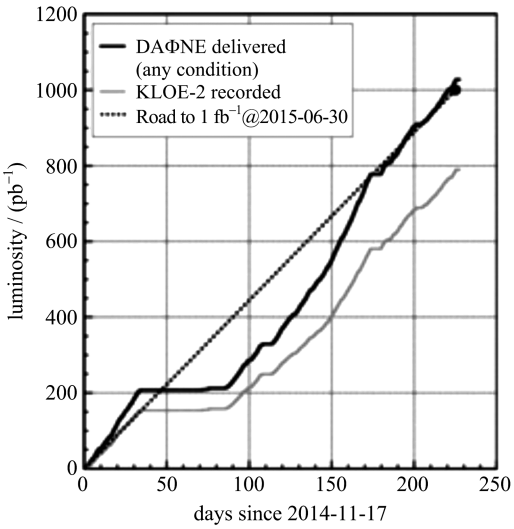

Fig. 1 Integrated luminosity collected by KLOE-2 since the start of the new data-taking

One of the main items of the KLOE-2 physics program[1] is the measurement of the Transition Form Factors (TFFs) of the pseudoscalar mesons both in the space-like and in time-like region of momentum transfer. The TFFs describe the coupling of mesons to photons and provide information about the nature of the mesons and their structure. Recently the interest in the TFFs has been renewed since they are an essential ingredient in the calculation of the hadronic light-by-light (LbL) scattering contribution to the anomalous magnetic moment of the muon[2]. The leading contribution to the LbL scattering is the single pseudoscalar exchange (Fig. 2), where the TFFs enter at the vertices connecting the pseudoscalar to photons.

The calculation of this contribution is model dependent since the exchanged meson is off-shell, and the TFFs for the off-shell meson are not measurable quantities. Nevertheless any experimental information, both for space - like and time-like q^2, can help in constraining the models used in the calculations. The TFFs at time-like q^2 can be studied by means of the Dalitz decays, like $\phi\to\eta e^+e^-$ and $\phi\to\pi^0 e^+e^-$.

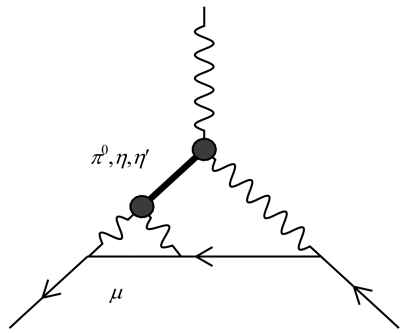

Fig. 2 Dominant contribution to the hadronic LbL scattering for the $(g-2)_\mu$ theoretical calculation

Another physics item that will be addressed by KLOE-2 is the $\gamma\gamma$ physics, i. e. processes like $e^+e^-\to e^+e^-\gamma^*\gamma^*\to e^+e^-X$, where X is a final state with even charge conjugation. The expected number of events as a function of the $\gamma\gamma$ energy $W_{\gamma\gamma}$ is

$$\frac{\mathrm{d}N}{\mathrm{d}W_{\gamma\gamma}}=L_{\mathrm{int}}\frac{\mathrm{d}F}{\mathrm{d}W_{\gamma\gamma}}\sigma_{\gamma\gamma\to X}$$

where L_{int} is the integrated luminosity, $\sigma_{\gamma\gamma\to X}$ the $\gamma\gamma$ cross-section, and $\frac{\mathrm{d}F}{\mathrm{d}W_{\gamma\gamma}}$ is the luminosity function which is plotted in Fig. 3 for three different energies. Since DAΦNE is operated at $\sqrt{s}\simeq M_\phi$, the accessible final state are either single pseudoscalar, $X=\eta,\pi^0$, or the double pion production, $X=\pi\pi$.

The cross-section for single pseudoscalar is

$$\sigma_{\gamma\gamma\to X}(q_1^2,q_2^2)=\frac{8\pi^2}{M_X}\Gamma(X\to\gamma\gamma)\mid F(q_1^2,q_2^2)\mid^2 \tag{2}$$

with $(q_1^2+q_2^2)=M_X^2$.

Then the radiative width $\Gamma(X\to\gamma\gamma)$ of the pseudoscalar meson, and the TFF $F(q_1^2,q_2^2)$ for space-like q^2 can be measured. Concerning the double pion final state, it is interesting to study the production of the lowest mass scalar meson $f_0(500)$, but it is also important for the new dispersive approach proposed for the hadronic LbL scattering[3].

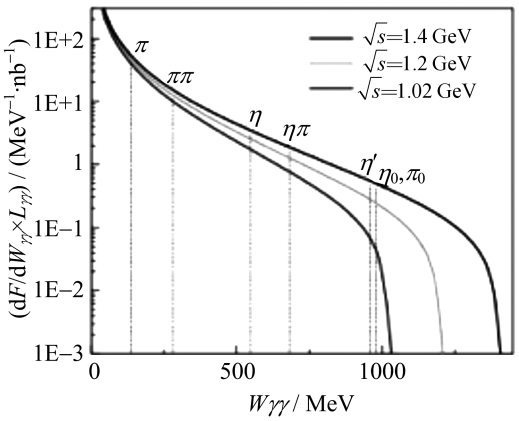

Fig. 3　Effective luminosity for γγ processes for three different energies

1　Detector upgrade

As a first step of the detector upgrade, a tagger system for scattered electrons and positrons in γγ processes had been installed already in 2010. It consists of two different devices: the Low Energy Tagger (LET) and the High Energy Tagger (HET), referring to the energy of the detected electrons or positrons (see Fig. 4).

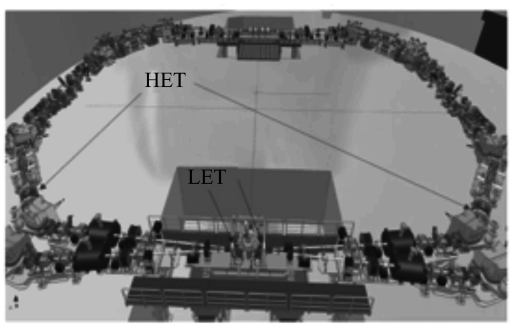

Fig. 4　Positioning of the taggers along the DAΦNE ring

During the 2013 shutdown an Inner Tracker[4] made of four layers of cylindrical triple GEM has been installed between the beam-pipe and the Drift Chamber, to improve the resolution for decay vertices close to the interaction point (IP), and to increase the acceptance for low momentum tracks. Furthermore two Crystal Calorimeters (CCALT)[5] have been added to cover the low polar angle regions to increase the acceptance for photons and $e^{\pm}$, originating from the IP, down to 10°, and finally the DAΦNE focusing quadrupoles, which are placed inside the KLOE detector, have been instrumented with calorimeters (QCALT)[6] made of tungsten and scintillator tiles.

1.1　The low energy tagger

The LET[7] has been designed to detect $e^{\pm}$ with energy between 150 and 350 MeV escaping from the beam-pipe, and it is placed at about 1 m from the IP. Since in this region there is no correlation between the energy and the scattering angle of the particles, a calorimetric device has been chosen. Then the LET consists of two calorimeters, each made of 4×5 LYSO crystals of 1.5×1.5×20 cm^3 dimensions. The crystals are read out by SiPM. The two calorimeters are placed symmetrically with respect to the IP, as shown in Fig. 5.

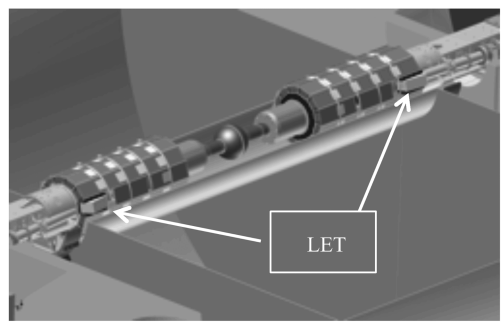

Fig. 5　Sketch of the LET calorimeter positioning

1.2　The high energy tagger

The HET[8] is designed to detect scattered $e^{\pm}$ of $E>400$ MeV. These particles escape the beam-pipe after the first bending dipole of DAΦNE, that can thus be used as spectrometer. The trajectories of the scattered electrons are strongly correlated with their energy. Then the HET is made of two scintillator hodoscopes readout by PMT, symmetrically placed 11 m far from the IP (Fig. 6).

The HET is acquired asynchronously with respect to the main KLOE detector, and for each KLOE trigger the HET information concerning three DAΦNE beam revolutions is stored. The synchronization is performed by using a machine signal. In Fig. 7 the time difference between the two HET stations is shown: the accelerator time

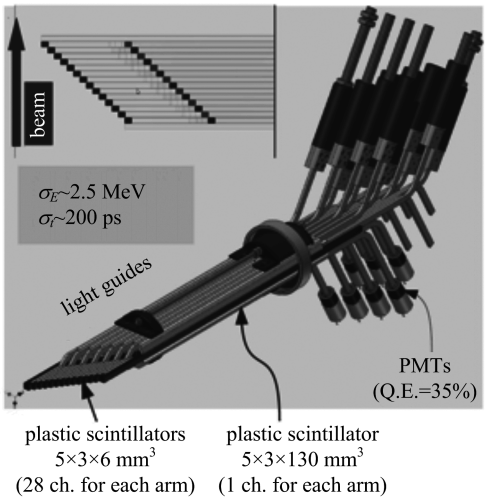

Fig. 6 Sketch of the HET hodoscope

structure of about 2.7 ns period is clearly visible. The superimposed histogram is the same distribution resulting from a run with separated beams in the IP, and shows that the level of background is less than 10%.

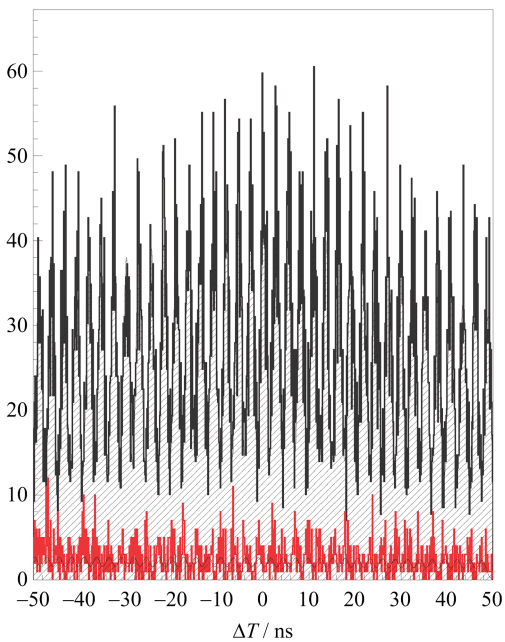

Fig. 7 Time difference between the two HET stations. Black: colliding beams; red: no collisions

2 $\gamma\gamma$ physics without taggers

With the KLOE data the two-photon width of the η meson has been measured by detecting events $e^+e^-\to e^+e^-\eta$, with $\eta\to\pi^+\pi^-\pi^0$ and $\pi^0\pi^0\pi^0$. The scattered leptons were not detected because the taggers were not present, then in order to suppress the large background from ϕ decays, the data collected off-peak, at $\sqrt{s}=1$ GeV, have been analyzed, corresponding to an integrated luminosity of 250 pb^{-1}. In Figs. 8 ~ 9 the distributions of the missing mass with respect to $\pi^+\pi^-\pi^0$ and $\pi^0\pi^0\pi^0$, respectively, are shown. By fitting these histograms we obtained the cross sections $\sigma(e^+e^-\to e^+e^-\eta)=(34.5\pm2.5\pm1.3)$ pb and $\sigma(e^+e^-\to e^+e^-\eta)=(32.0\pm1.5\pm0.9)$ pb for the charged and neutral η decay channel, respectively. By combining them, $\sigma(e^+e^-\to e^+e^-\eta)=(32.7\pm1.3\pm0.7)$ pb, from which we extract the most precise measurement to date of the two-photon width: $\Gamma(\eta\to\gamma\gamma)=(520\pm20\pm13)$eV[9].

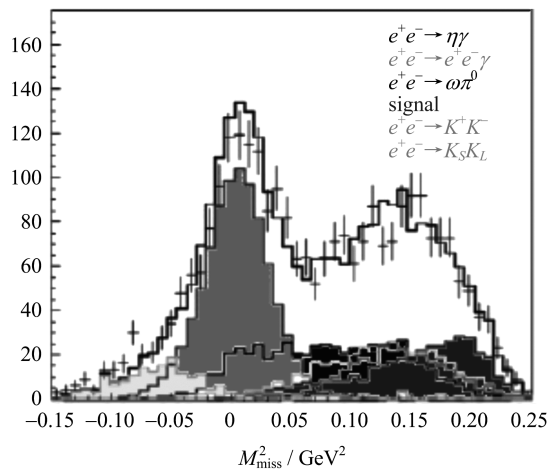

Fig. 8 $\gamma\gamma\to\eta\to\pi^+\pi^-\pi^0$

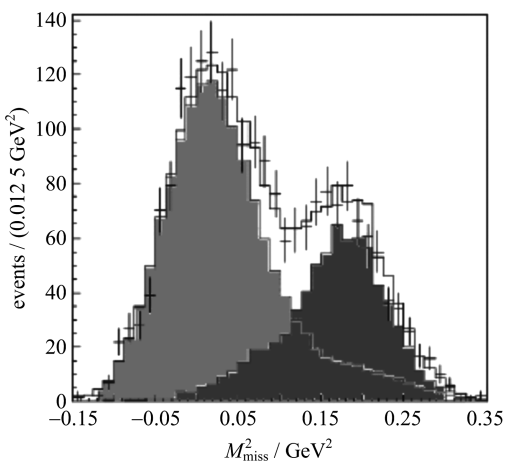

Fig. 9 Dark grey: $\gamma\gamma\to\eta\to\pi^0\pi^0\pi^0$; light grey: $e^+e^-\to\eta\gamma$ with $\eta\to\pi^0\pi^0\pi^0$

3 Prospects for γγ physics with taggers

Since the KLOE-2 data-taking is performed at the ϕ peak, the detection of the scattered electrons and positrons in the tagging stations will be essential for closing the kinematics of the events and thus reduce the large background coming from ϕ decays.

3.1 $\gamma\gamma \to \pi^0$

The radiative width of the π^0 has been calculated in Chiral Perturbation Theory with 1.4% uncertainty, $\Gamma(\pi^0 \to \gamma\gamma) = (8.09 \pm 0.11)$ eV[10], and from the experimental point of view, the most precise measurement up to now comes from the PrimEx Collaboration and is based on the Primakoff effect, $\Gamma(\pi^0 \to \gamma\gamma) = (7.82 \pm 0.14 \pm 0.17)$ eV[11]. However the measurements based on Primakoff effect suffer from some model dependence due to the conversions in the nucleus field. At KLOE-2 the π^0 width can be measured with a different process by selecting $e^+e^- \to e^+e^-\pi^0$ events with quasi-real photons ($q^2 \simeq 0$). These events are selected by requiring that the scattered $e^\pm$ go in the two HET stations, and the two photons from π^0 decay are detected in the calorimeter. According to the Monte Carlo (MC) simulation the double HET coincidence efficiency is 1.4%. Then for a cross-section $\sigma(e^+e^- \to e^+e^-\pi^0) = 0.28$ nb, about 2 000 events/fb^{-1} are expected, allowing to reach a 1% accuracy in $\Gamma(\pi^0 \to \gamma\gamma)$ with 5 fb^{-1} of integrated luminosity.

Moreover the $\pi^0\gamma^*\gamma$ TFF with a quasi-real photon and a virtual one can also be measured, by selecting events in which one electron is detected in the HET ($q^2 \simeq 0$) and the other one at a large angle in the KLOE main detector. In this way a still unexplored q^2 region ($|q^2| < 0.1$ GeV^2, see Fig. 10), which is important to constrain the TFF parametrizations, can be investigated.

3.2 $\gamma\gamma \to \pi^0\pi^0$

In Fig. 11 is shown the four photon invariant mass distribution from a preliminary analysis performed on the old KLOE data sample; there is a clear excess of events, with respect to all known background sources, at low mass values.

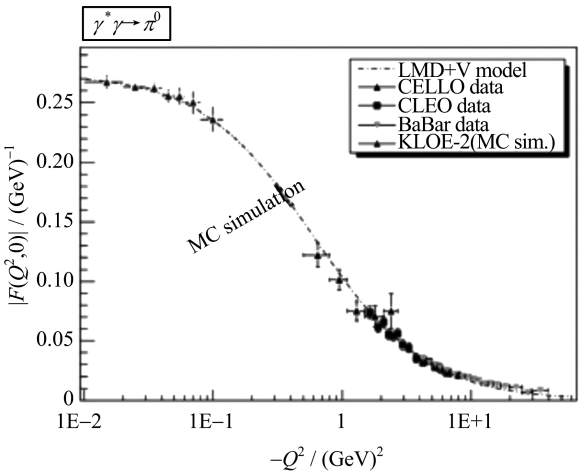

Fig. 10　TFF as a function of q^2. The KLOE-2 points are from a MC simulation

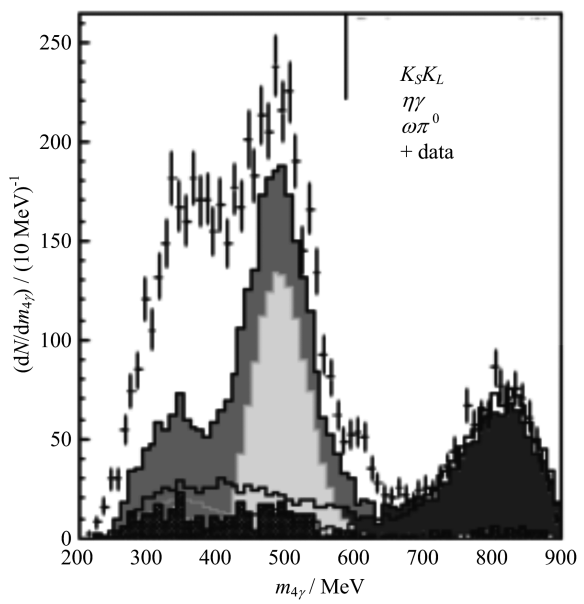

Fig. 11　Off-peak KLOE data sample: four photon invariant mass for $e^+e^- \to e^+e^-\pi^0\pi^0$, the top solid histogram is the sum of all the background processes

However, since it is impossible to close the kinematics due to the absence of the taggers, the residual background is of difficult evaluation. The measurement of the $e^+e^- \to e^+e^-\pi^0\pi^0$ cross section will be possible with the KLOE-2 data, where the relevant energy region can be covered by selecting events with either LET-LET or HET-LET coincidences.

4 Transition form factor measurements in Dalitz decays

The TFFs measured in Dalitz decays are functions of the four-momentum squared $q^2 = m^2_{l^+l^-}$, and according to Vector Meson Dominance (VMD) are usually parametrized as $F(q^2) = 1/\left(1-\frac{q^2}{\Lambda^2}\right)$, where Λ is a characteristic mass, identified with the nearest vector meson. The dilepton invariant mass distributions of $\eta \to e^+ e^- \gamma$ and $\eta \to \mu^+ \mu^- \gamma$, measured by NA60[12] and by the A2 Collaboration at MAMI[13-14] are described by $\Lambda_\eta^{-2} = 1.92 \sim 1.95\ \mathrm{GeV}^{-2}$ in agreement with the VMD predictions $\Lambda_\eta^{-2} = 1.88\ \mathrm{GeV}^{-2}$, but the TFF of $\omega \to \pi^0 \mu^+ \mu^-$, also measured by NA60, is not well reproduced by VMD, $\Lambda_\omega^{-2} = 2.24\ \mathrm{GeV}^{-2}$, but the VMD expectation is $1.68\ \mathrm{GeV}^{-2}$. To explain this behaviour other models have been proposed[15-17], that predict deviations from VMD also for $\phi \to \eta(\pi^0) l^+ l^-$.

4.1 $\phi \to \eta e^+ e^-$

The TFF slope for $\phi \to \eta e^+ e^-$ was measured with low statistics by the SND Collaboration at Novosibirsk, $\Lambda_\phi^{-2} = (3.8 \pm 1.8)\ \mathrm{GeV}^{-2}$[18]. This value is compatible, due to its large uncertainty, with the VMD expectation $\Lambda_\phi^{-2} \simeq m_\phi^{-2} \simeq 1\ \mathrm{GeV}^{-2}$. At KLOE $1.7\ \mathrm{fb}^{-1}$ of data have been analyzed looking for $\phi \to \eta e^+ e^-$ with $\eta \to \pi^0 \pi^0 \pi^0$. The $m_{e^+e^-}$ distribution is shown in Fig. 12.

From the event counting the branching ratio can be obtained:

$$Br(\phi \to \eta e^+ e^-) = (1.075 \pm 0.007 \pm 0.038) \times 10^{-4}$$[19].

The slope $b = \Lambda_\phi^{-2}$ is then extracted from a fit of the distribution of the $e^+ e^-$ invariant mass to the parametrization from Ref. [20], by using the one-pole formula for the TFF. We obtain a value, $b = (1.17 \pm 0.10^{+0.07}_{-0.11})\ \mathrm{GeV}^{-2}$[19], which is consistent with the VMD predictions. The TFF as a function of the $e^+ e^-$ invariant mass is shown in Fig. 13.

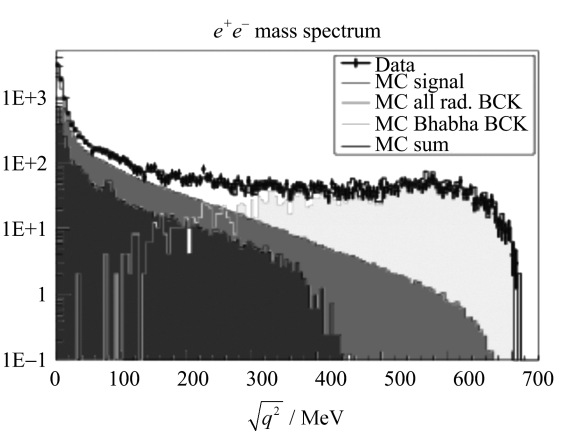

Fig. 12 $e^+ e^-$ **invariant mass for** $\phi \to \eta e^+ e^-$

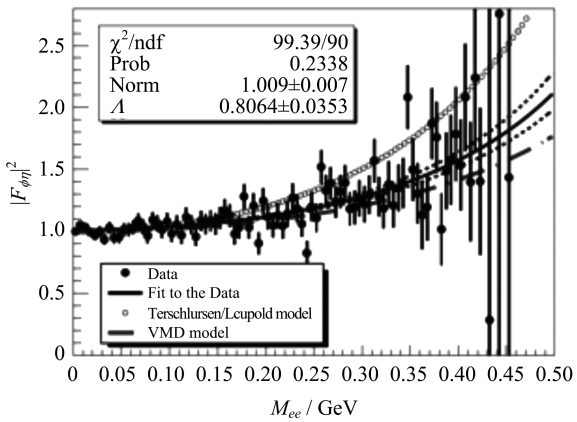

Fig. 13 **TFF as a function of the** $e^+ e^-$ **invariant mass, compared with different theoretical predictions**

4.2 $\phi \to \pi^0 e^+ e^-$

The decay $\phi \to \pi^0 e^+ e^-$ has been studied by the Novosibirsk experiments CMD-2 and SND that reported $Br(\phi \to \pi^0 e^+ e^-) = (1.22 \pm 0.34 \pm 0.21) \times 10^{-5}$[21] and $(1.01 \pm 0.28 \pm 0.29) \times 10^{-5}$[22], respectively, but no measurement has been published on the TFFs slope.

In the sample of $1.7\ \mathrm{fb}^{-1}$ of KLOE data, about 9 000 events for this decay have been selected. In Fig. 14 the data-MC comparison is shown for the $e^+ e^-$ invariant mass, and in Fig. 15 for the two photon invariant mass. The residual background, mainly coming from radiative Bhabha scattering, is subtracted by fitting the distribution of the recoil mass against the $e^+ e^-$ pair.

The TFF as a function of the $e^+ e^-$ invariant mass is obtained after the background subtraction and in Fig. 16 is compared with the theoretical expectations. It shows a good agreement with the model of Ref. [17]. From the subtracted invariant

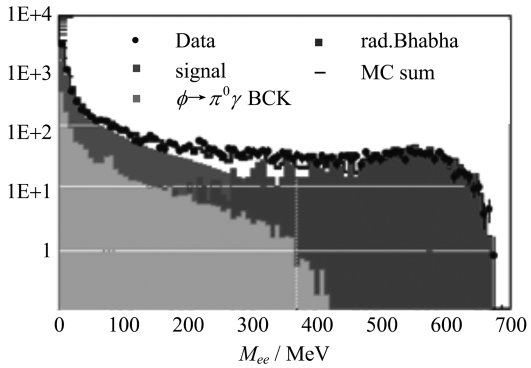

Fig. 14　$e^+ e^-$ **invariant mass distribution for** $\phi \to \pi^0 e^+ e^-$

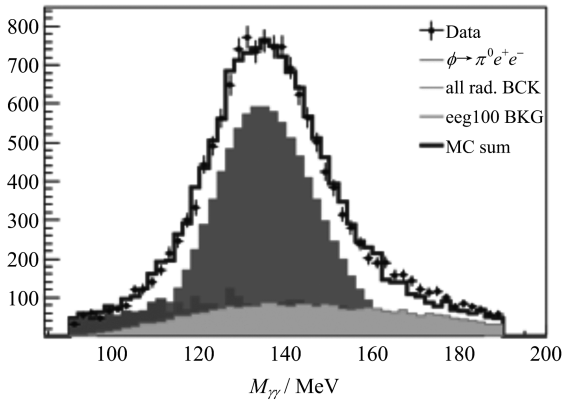

Fig. 15　**Two photon invariant mass distribution for** $\phi \to \pi^0 e^+ e^-$

mass spectrum the branching ratio also can be derived,

$$Br(\phi \to \pi^0 e^+ e^-) = (1.19 \pm 0.05^{+0.05}_{-0.10}) \times 10^{-5}$$

for $m_{ee} < 700$ MeV. Higher values of the invariant mass are not accessible due to the selection of the events; however the branching ratio for all the invariant mass range can be extrapolated according to the model of Ref. [17],

$$Br(\phi \to \pi^0 e^+ e^-) = (1.35 \pm 0.05^{+0.05}_{-0.10}) \times 10^{-5}.$$

5　Conclusion

The KLOE Collaboration is continuing to exploit the high statistics sample of light mesons collected during the first phase of the experiment, to perform precision measurements in hadron physics. The most accurate measurement up to now of the η width in $\gamma\gamma$, $\Gamma(\eta \to \gamma\gamma) = (520 \pm 20 \pm 13)$ eV, has been obtained.

From the study of the ϕ Dalitz decays, the branching ratios and the Transition Form Factors

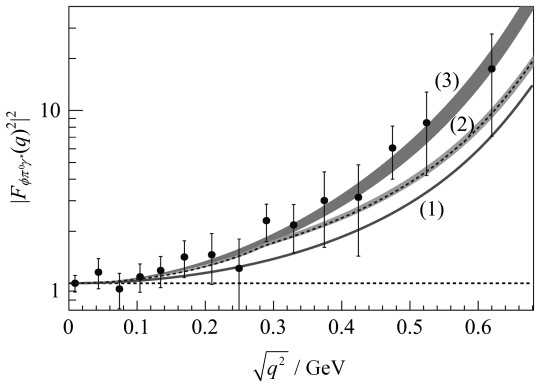

Fig. 16　$\phi \to \pi^0 e^+ e^-$ **: TFF as a function of** $e^+ e^-$ **invariant mass, compared with the following theoretical predictions, (1): VDM, (2)-grey band: Ref. [16], (2)-dashed line: Ref. [23], (3): Ref. [17]**

of $\phi \to \eta e^+ e^-$ and $\phi \to \pi^0 e^+ e^-$ have been measured.

The KLOE-2 data-taking, with the upgraded detector, is in progress, with the goal to collect at least 5 fb^{-1} in the years to come. A rich program of measurements has been proposed[1]. Among these measurements a special place, due to the new taggers, is occupied by the $\gamma\gamma$ production of pseudoscalar mesons, which can help to shed light on some of the still puzzling questions in this field.

References

[1] AMELINO-CAMELIA G, ARCHILLI F, BABUSCI D, et al. Physics with the KLOE-2 experiment at the upgraded DAΦNE[J]. Eur Phys J C, 2010, 68: 619-681.

[2] JEGERLEHNER F, NYFFELER A. The muon $g-2$ [J]. Phys Rept, 2009, 477: 1-110.

[3] COLANGELO G, HOFERICHTER M, PROCURA M, et al. Dispersion relation for hadronic light-by-light scattering: theoretical foundations[J]. JHEP, 2015, 09: 074.

[4] BALLA A, BENCIVENNI G, BRANCHINI P, et al. The cylindrical GEM detector for the KLOE-2 Inner Tracker[J]. JINST, 2014, 9: C01014

[5] CORDELLI M, DANè E, GIOVANNELLA S, et al. CCALT: A crystal CALorimeter with timing for the KLOE-2 upgrade[J]. Nucl Instrum Meth A, 2013, 718: 81-82.

[6] CORDELLI M, CORRADI G, HAPPACHER F, et al. QCALT: A tile calorimeter for KLOE-2 experiment [J]. Nucl Instrum Meth A, 2010, 617: 105-106.

[7] BABUSCI D, BINI C, CIAMBRONE P, et al. The

low energy tagger for the KLOE-2 experiment[J]. Nucl Instrum Meth A, 2010, 617: 81-84.

[8] ARCHILLI F, BABUSCI D, BADONI D, et al. Gamma-gamma tagging system for KLOE2 experiment [J]. Nucl Instrum Meth A, 2010, 617: 266-268.

[9] BABUSCI D, BADONI D, BALWIERZ-PYTKO I, et al (KLOE-2 Collaboration). Measurement of η meson production in $\gamma\gamma$ interactions and $\Gamma(\eta\to\gamma\gamma)$ with the KLOE detector[J]. JHEP, 2013, 01: 119.

[10] KAMPF K, MOUSSALLAM B. Chiral expansions of the π^0 lifetime[J]. Phys Rev D, 2009,79: 076005.

[11] LARIN I, MCNULTY D, CLINTON E, et al (PrimEx). New measurement of the π^0 radiative decay width[J]. Phys Rev Lett, 2011, 106: 162303.

[12] URAS A (for the NA60 Collaboration). Measurement of the η and ω Dalitz decays transition form factors in p-A collisions at 400 GeV/c with the NA60 apparatus [J]. J Phys Conf Ser, 2011, 270: 012038.

[13] BERGHÄUSER H, METAG V, STAROSTIN A, et al. Determination of the η-transition form factor in the $\gamma p\to p\eta\to p\gamma e^+e^-$ $\gamma p\to p\eta\to p\gamma e^+e^-$ reaction[J]. Phys Lett B, 2011, 701: 562-567.

[14] AGUAR-BARTOLOME P, ANNAND J R M, Arends H J, et al (A2 Collaboration). New determination of the η transition form factor in the Dalitz decay $\eta\to e^+e^-\gamma$ with the Crystal Ball/TAPS detectors at the Mainz Microtron[J]. Phys Rev C, 2014, 89: 044608.

[15] TERSCHLÜSEN C, LEUPOLD S. Electromagnetic transition form factors of mesons[J]. Prog Part Nucl Phys, 2012, 67: 401-405.

[16] SCHNEIDER S P, KUBIS B, NIECKNIG F. $\omega\to\pi^0\gamma^*$ and $\phi\to\pi^0\gamma^*$ transition form factors in dispersion theory[J]. Phys Rev D, 2012, 86: 054013.

[17] IVASHYN S. Vector to pseudoscalar meson radiative transitions in chiral theory with resonances[J]. Prob Atomic Sci Technol, 2012, N1: 179-182

[18] ACHASOV M N, AULCHENKO V M, BELOBORODOV K I, et al. Study of conversion decays $\phi\to\eta e^+e^-$ and $\eta\to\gamma e^+e^-$ in the experiment with SND detector at VEPP-2M collider[J]. Phys Lett B, 2001, 504: 275-281.

[19] BABUSCI D, BALWIERZ-PYTKO I, BENCIVENNI G, et al. (KLOE-2) Study of the Dalitz decay $\phi\to\eta e^+e^-$ with the KLOE detector[J]. Phys Lett B, 2015: 742: 1-6.

[20] LANDSBERG L. Electromagnetic decays of light mesons[J]. Phys Rept, 1985, 128: 301-376.

[21] AKHMETSHIN R R, ANASHKIN E V, ARPAGAUS M, et al (CMD-2). Observation of the conversion decay $\phi\to\pi^0e^+e^-$ at CMD-2[J]. Phys Lett B, 2001, 503: 237-244.

[22] ACHASOV M N, BELOBORODOV K I, BERDYUGIN A V, et al. Measurement of the $\phi\to\pi^0e^+e^-$ decay probability[J]. JETP Lett, 2002, 75: 449-451(Pisma Zh Eksp Teor Fiz, 2002, 75: 539-541).

[23] DANILKIN I V, FERNANDEZ-RAMIREZ C, GUO P, et al. Dispersive analysis of $\omega/\phi\to3\pi,\pi\gamma$[J]. Phys Rev D, 2015, 91: 094029.